Hindawi
International Journal of Antennas and Propagation
Volume 2021, Article ID 9991748, 13 pages
https://doi.org/10.1155/2021/9991748

Research Article

Compact Dual-Band Circularly Polarized Stacked Patch Antenna for Microwave-Radio-Frequency Identification Multiple-Input-Multiple-Output Application

Enze Zhang,[1] **Andrea Michel**,[2] **Paolo Nepa**,[2] **and Jinghui Qiu**[1]

[1]*School of Electronics and Information Engineering, Harbin Institute of Technology, Harbin 150001, China*
[2]*Department of Information Engineering, University of Pisa, 56122 Pisa, Italy*

Correspondence should be addressed to Enze Zhang; zez1992@foxmail.com

Received 21 March 2021; Accepted 18 May 2021; Published 29 May 2021

Academic Editor: Stefania Bonafoni

A compact, low-profile, two-port dual-band circularly polarized (CP) stacked patch antenna for radio-frequency identification (RFID) multiple-input-multiple-output (MIMO) readers is proposed, which employs the shared-aperture technique. The proposed antenna adopts a 1.524 mm thickness Rogers Ro4350b substrate with relative permittivity of 3.48. Two pairs of isolated ports are working at two microwave- (MW-) RFID bands (2.4–2.485 GHz and 5.725–5.875 GHz) with high port isolation of 25 dB and 30 dB, respectively. A shared metal slot layer is designed to separate two feeding structures of the lower band and upper band for port isolation enhancement as well as saving space. Corner-truncated square slot and patch configurations have been designed to obtain CP modes. In the lower and upper MW-RFID bands, the relative impedance bandwidths are 12.2% and 5.7%, and the maximum realized gains are higher than 7.3 dBic. Moreover, two-element configurations have been combined for an RFID MIMO system that occupies a dimension of 119 mm × 119 mm × 12.9 mm. The MIMO antenna performance of envelope correlation coefficient (ECC) is lower than 0.03, and diversity gain is close to 10 dB.

1. Introduction

In recent years, radio-frequency identification (RFID) technology has obtained significant attention due to its practical and low-cost labeling performance. It has been employed in the fields of biomedicine, transportation, logistics, and so on. The frequency bands assigned to the RFID technology are 125/135 kHz (low-frequency (LF) band), 13.56 MHz (high-frequency (HF) band), 433/860–960 MHz (ultrahigh-frequency (UHF) band), and 2.45/5.8 GHz (microwave (MW) band). Among them, the MW-RFID system has been a popular research tendency on account of its high transmission rate and long transmission distance as well as compact structure, especially in the field of active RFID technique. Since the RFID reader antenna always needs to work at different frequencies, accommodating two working bands in one RFID reader antenna has been a critical need to increase compact dimension efficiency.

Since RFID reader antenna usually needs to operate at multiple frequencies, combining two operating bands in one RFID antenna has been a critical need to increase efficiency in compact dimension. The dual-band ((federal communications commission ultrahigh frequency) FCC UHF and MW bands) antennas that have been proposed in [1–4] apply for linear polarization (LP). In [1], the design employs an aperture patch to achieve dual-band radiation. A ring plate with curved slots is designed in [2]. Finally, aperture-fed and marquise-brilliant-diamond-shaped (MBDS) structures are designed in [3, 4].

Moreover, due to the RFID tag detection regardless of the physical orientation, circular polarization is favorite at both the RFID working bands. So far, kinds of dual-band circularly polarized (CP) solutions have been proposed. Most of them are achieved by employing corner-chamfered stacking square patches [5–7] or slot-loading patches [8]. In [9], two concentric ring radiating elements were excited with coupling apertures and exhibited a general area of $\lambda/2 \times \lambda/$

$2 \times \lambda/40$. Nevertheless, these one-feed antennas suffered from a narrow impedance bandwidth. Dual-band CP antennas with two feeds at separate frequencies are reported in [10–14]. In [10–13], traditional hybrid couplers and multi-radiating elements are used for dual-CP antenna configurations for wide bandwidth and low mutual coupling. However, they all need large antenna dimensions, especially for antenna arrays. Two corner-truncated stacking square patches and three low loss dielectric layers are employed in [14] to obtain excellent performance of impedance bandwidth as well as axial ratio (AR) in a compact dimension. However, its AR bandwidth in a high-frequency band (7 GHz) is narrow (0.1 GHz). In [15], four inverted-F radiating elements and a 90° phase hybrid coupler are used for the UHF-RFID application. In comparison, a CP patch is placed in the center of the four inverted-F monopoles for the 2.45 GHz wireless local area network (WLAN) application. It occupied a compact volume of $0.5 \times 0.5 \times 0.05\lambda^3$, but its gain of both operating bands is lower than −0.6 and 1.2 dBic, respectively.

Currently, the RFID system has started to focus on employing multiple radiating elements at both reader and tag. Compared with the single-input-single-output (SISO) system, the multiple-input-multiple-output (MIMO) system effectively enhances the RFID cover area, solves the non-line-of-sight (NLoS) problem, increases the stability of data transmission, and improves the RFID information-carrying capacity.

Multiple antenna elements have been firstly used for RFID tags and readers [16]. In [17], the SISO RFID and MIMO RFID channel's multipath fading have been measured and discussed. Employing the MIMO technique in the RFID system can obtain the enhancement of the fading depth. A distributed antenna system (DAS) for RFID has been designed to compare with conventional single-antenna RFID system [18]. Multiple transmitting and receiving antenna elements as a reader locate in different places. When the DAS RFID system works in a 10 m^2 space, it can obtain a successful reading rate of 100%. In comparison, the conventional RFID SISO system's reading rate is lower than 60%. In [19], a 2×2 MIMO frontend for an RFID MIMO application in the UHF band has been proposed to verify the RFID MIMO system advantage of beamforming and diversity combining as well as localization at the RFID reader.

This paper proposes a compact, low-cost, dual-port dual-band CP antenna for MW-RFID MIMO application. It is suitable for operating at both 2.45 GHz and 5.8 GHz MW-RFID bands. Significantly, the $0.5 \times 0.5 \times 0.1\lambda^3$ single radiating element consists of a stacked corner-truncated patch electromagnetically activated with square ring slots. The novelties of the design have been concluded as follows:

(i) The advantages of operating in higher RFID frequency bands include broad reading coverage, fast reading speed, and extensive information storage ability. When the RFID systems' working band increases to the MW range (2.45/5.8 GHz), the RFID reader antenna's design will be more acute and complicated. Some dual-band RFID antennas working at MW bands (2.45/5.8 GHz) have been proposed in [20–23]. However, all of them are designed for LP with a single feed. Because these two standards operating frequencies (2.45 and 5.8 GHz) need to work simultaneously in one system, the proposed dual-feed dual-band CP antenna can eliminate the use of single-port dual-band antennas. Moreover, compared with LP antennas, the CP antenna has many superiorities such as insensitivity to antenna orientations, reduced multipath fading, and adaption to harsh climatic conditions for RFID MIMO application.

(ii) A novel dual-port feeding technique has been designed in this antenna. Unlike other stacked patch antenna solutions, these two feed lines are separated on both sides of the Rogers Ro4350b laminates (the lower and upper band feed lines have been placed on the bottom and top sides of the laminates, resp.). A metal layer with a square ring slot is stuck in the middle of the laminates as a coupling slot for the lower band feed line and a ground plane for the upper band feed line. Using this shared metal slot layer structure can decrease the interference between these two feed lines and make dimensions more compact.

(iii) Dual-band antennas operating at MW-RFID 2.45/5.8 GHz bands are essential for portable readers. The RFID reader operating at the MW band can transmit collected data to a data processor with WLAN. Moreover, this antenna can also further apply the Bluetooth and Wi-Fi field for industrial, scientific, and medical (ISM) bands.

The specific structure of the proposed antenna element is explained in Section 2. The MIMO antenna prototype is designed, and its numerical and measured results are proposed and discussed in Section 3. Conclusions are proposed in Section 4.

2. Design of the Antenna Element

Figure 1 proposes the slot-fed stacked antenna's layout that consists of two 1.53 mm thickness Rogers Ro4350b laminates ($\varepsilon_r = 3.48$; $\tan\delta = 0.0037$) separated with a metal slot layer. The microstrip feed line working at the lower MW-RFID frequency band is printed on the bottom side of the lower laminate, and the microstrip feed line working at the upper MW-RFID frequency band is printed on the top side of the upper laminate.

In 1985, Pozar firstly designed aperture coupling feed [24], which has the advantages of antenna bandwidth enhancement. Coupling of the slot to the patch and the feed line is obtained due to the longitudinal current flow's slot interruption [25]. A ring slot structure has been designed to be coupled with the patch antenna [26–28]. Particularly in [26, 27], dual-port LP antennas fed with square ring slots

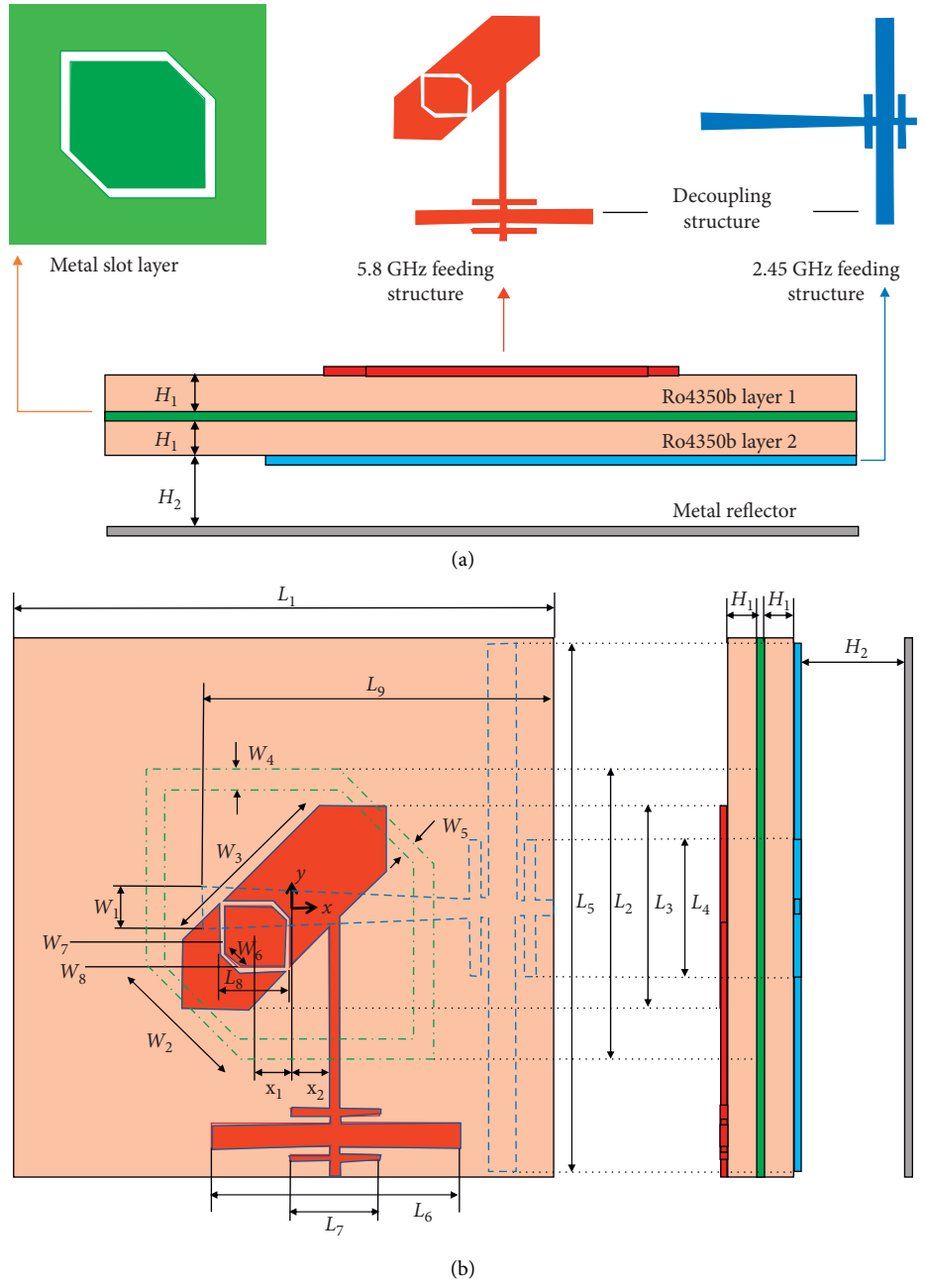

Figure 1: Antenna structure: (a) stack-up structure; (b) top view and side view.

have been designed. Four two-port LP aperture-shared antennas are then discussed in [28] with a sequentially rotated feed technology for sound CP purity radiation. However, the extensive feeding network's dimension limits the antenna compactness. In this paper, CP fields have been achieved with the corner-truncated two-port slots and patch instead of bulky feeding networks.

For the 2.45 GHz MW-RFID frequency band, as in square ring slot-coupling feeding techniques, the square ring slot with side length L_2 close to $\lambda_{2.45}$ has been etched in the metal layer. The printed microstrip feed line placed on the lower laminate's bottom side was used to feed the slot at two consecutive edges. The $L_3 \times L_3$ square radiating patch was then printed on the upper laminate's top side. Its side is slightly less than $\lambda_{2.45}/2$ to achieve a bit different resonating frequency.

For the 5.8 GHz MW-RFID frequency band, the microstrip line has been connected with the top-side radiation patch. And the square ring slot which side length is about $\lambda 5.8$ has been etched in the center of the top-side patch. As shown in Figure 1, the metal layer with a square slot can be seen as a ground plane of 5.8 GHz radiating structure. Compared with the 5.8 GHz coupling slot dimension of $L_8 \times L_8$, the 2.45 GHz coupling slot has a too much larger size of $L_2 \times L_2$ to disturb the working of the 5.8 GHz coupling slot and deteriorate the antenna performance at the 5.8 GHz MW-RFID band.

The surface current distributions at 5.8 GHz operating mode and 2.45 GHz operating mode are shown in Figure 2. At 5.8 GHz operating mode, Port 1 is activated, and the coupling area is mainly located at the patch's small slot. At 2.45 GHz operating mode, Port 2 is activated, and its coupling area is the large slot and the edge of the patch. Two decoupling feeding structures are employed to enhance port isolation. We can find that the coupling between these two ports is very slight. That is also confirmed by Figure 3, which presents the S-parameters' curves of employing the decoupling structure (DS) and not employing the DS. As shown in Figure 3, after employing DS, the isolation increases from 5 to 23 dB and 7 to 30 dB. Simultaneously, the impedance bandwidth also increases by 50 MHz and 100 MHz at 2.45/5.8 MW-RFID bands, respectively.

Moreover, two opposite corners of the square ring slots and radiating patch are chamfered as a corner-truncated structure. Hence, an asymmetry is proposed in the square ring slots and patch to excite CP at both ports [29, 30].

In the end, a metal reflector is added at a distance of H_1 from the lower substrate's bottom to decrease the back-radiation and enhance the broadside gain during the 2.45 GHz MW-RFID frequency band. In comparison, the metal slot layer could be seen as the metallic reflector for the 5.8 GHz radiating structure. In Table 1, the geometrical parameters have been optimized to achieve impedance bandwidth and port isolation requirements in the 2.45/5.8 GHz MW-RFID working bands.

A prototype of the dual-band CP MW-RFID antenna has been fabricated for validation, and its photos of two Rogers Ro4350b layers are shown in Figure 4. As shown in Figure 5, the simulated and measured S-parameters meet a good agreement. The measured 10-dB impedance bandwidths are in the ranges 2.36–2.67 GHz (12.7%) and 5.64–5.94 GHz (5.1%), which cover entirely MW-RFID frequency band (2.4–2.485/5.725–5.875 GHz). The isolation of higher than 25 dB and 30 dB is obtained in the lower and upper MW-RFID band, respectively.

In the center of Figure 6, the fabricated prototype is measured in the anechoic chamber at the Harbin Institute of Technology measurement facilities. As shown in Figure 6, the measured radiation patterns (RP) (for both ports, RHCP has been considered) are compared with simulated results at the *XZ* and *YZ* planes, at 2.45 GHz and 5.8 GHz, respectively. The half-power bandwidths (HPBWs) are about 60° in both *XZ* and *YZ* planes, at 2.45 GHz. The central-asymmetric feeding structure leads to an asymmetric RP around the broadside (*z*-axis) at 5.8 GHz. The HPBWs are about 44° and 47° in *XZ* and *YZ* planes, respectively, at 5.8 GHz. In Figure 7, the maximum measured realized gain in the broadside direction is 7.4 dBic in both 2.45 GHz and 5.8 GHz MW-RFID bands.

The AR at the broadside direction is shown in Figure 8. The simulated and measured AR at 2.45/5.8 GHz MW-RFID frequency band meet agreement. The 3 dB AR bandwidths almost cover MW-RFID bands except for a 0.3 dB deterioration at 2.45 GHz. The AR variations with respect to the θ-angle at 2.45 GHz and 5.8 GHz are proposed in Figures 9 and 10, respectively. In the 2.45 GHz MW-RFID band, the simulated and measured results meet good agreement. The measured 3 dB AR beamwidth is over 70° around the broadside. However, due to the surface-wave diffraction at the laminate's borders [13], the cross-polar level is somewhat higher in the 5.8 GHz MW-RFID band than expected, with deterioration around $\theta = +/- 25°$. Thus, the measured 3 dB AR beamwidth is 40°. The diffraction also appears in the 2.45 GHz MW-RFID band, but it is less severe since the dielectric layer is relatively thinner at the lower operating band. If the proposed configuration is employed on a large substrate, the effect of diffraction will be decreased. Thus, a trade-off between the compact dimension and AR beamwidth has been taken into account to guarantee an acceptable RFID tag reading range. Moreover, the electromagnetic band-gap (EBG) technique could reduce surface waves' effect [31].

Table 2 compares the proposed antenna element with other solutions for dual-band CP antenna designs. The proposed design achieves excellent isolation (>23 dB) and realized gain (5 dBic) with a single radiation element and no complicated feeding network. Its compact structure results in being a good choice for dual-band RFID MIMO applications.

3. Application for MIMO System

The proposed antenna element is then used in the MIMO system. As shown in Figure 11, the second antenna element is employed and rotated 90°. Thus, the four SMA connector ports have been placed at the edges of the configuration for a simple connection with feed lines. As a trade-off between low ECC and compact dimension, the two antenna elements are constructed at a distance of D = 59 mm. In order to decrease the mutual coupling between these two antenna elements, three slot gaps are etched in the metal slot layer, and one rectangular metal ring is printed on the bottom side of the lower laminate.

The simulated and measured reflection coefficients are proposed in Figure 12. The 10 dB impedance bandwidths can cover both 2.45 GHz and 5.8 GHz MW-FRID bands. Due to the low mutual coupling between antenna elements, the MIMO antenna's impedance matching performance has a slight difference compared with the single element, especially in the 5.8 GHz RFID band. As shown in Figure 13, thanks to the slot gaps and rectangular metal ring, the measured port isolation is higher than 23 dB (because of the same element configuration, S_{21} and S_{43} are almost the same), which shows good agreement with simulation results.

As shown in Figure 14, the simulated and measured RP in the MIMO configuration meets good agreement. In both *XZ* and *YZ* planes, the HPBWs are larger than 65° and 60° at 2.45 GHz (Port 1 and Port 3) and 35° and 34° at 5.8 GHz (Port 2 and Port 4). Thanks to the low element mutual interference, the RP in MIMO configuration just appears slightly deterioration at 5.8 GHz compared with the RP of the single-antenna element in Figure 6. In the MIMO configuration, the maximum measured realized gains in the broadside direction are 5.7 and 6.5 dBic (Port 1 and Port 3)

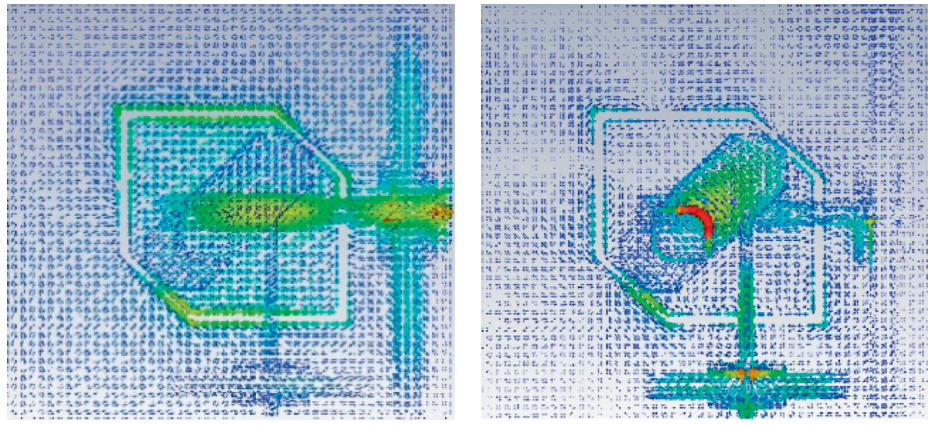

(a) (b)

Figure 2: Surface current in (a) 2.45 GHz and (b) 5.8 GHz operating mode.

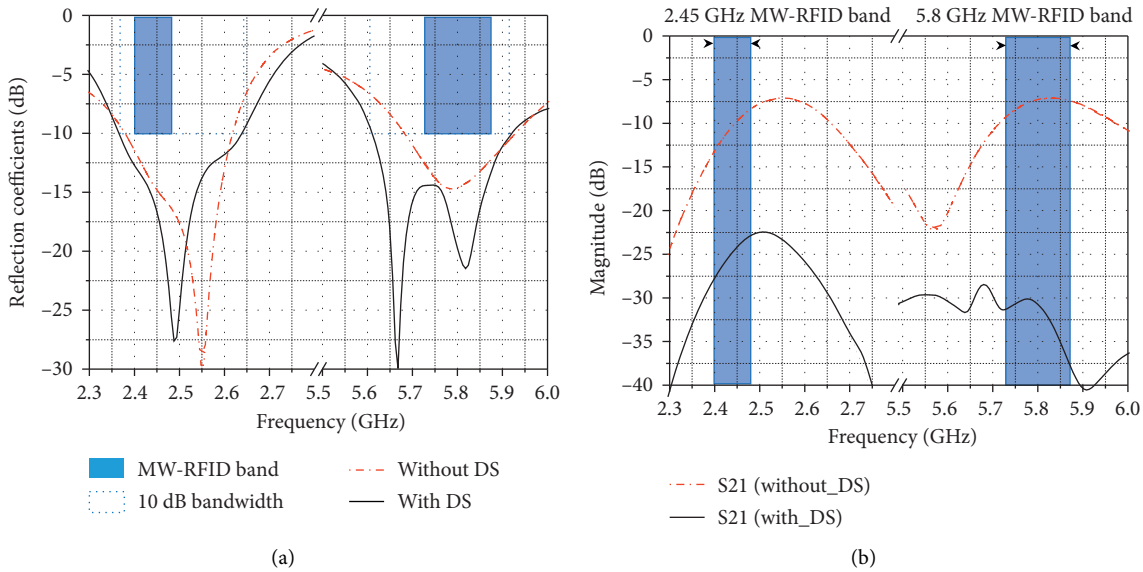

(a) (b)

Figure 3: (a) Reflection coefficients and (b) mutual coupling of the antenna with decoupling structure (DS) and without DS.

in the 2.45 GHz MW-RFID band and 7.7 and 8.7 dBic (Port 2 and Port 4) in the 5.8 GHz MW-RFID band, respectively.

Figure 15 shows great agreement between simulated and measured AR in the MIMO configuration. And the measured 3 dB AR bandwidth covers both 2.45 GHz and 5.8 GHz MW-RFID bands. Because of the good isolation proposed in Figure 13, the AR performances of the single-antenna element (shown in Figure 8) and MIMO configuration are almost the same.

The envelope correlation coefficient (ECC) and diversity gain (DG) are the MIMO system's critical performance index. Considering the affection of the antenna's spatial behavior, the ECC can be evaluated from the far-field RP by (1) and (2) [32].

$$\rho_e = \frac{\left| \iint_{4\pi} \left[\overrightarrow{E_1}(\theta,\phi) \cdot \overrightarrow{E_2}(\theta,\phi) d\Omega \right] \right|^2}{\iint_{4\pi} \left| \overrightarrow{E_1}(\theta,\phi) \right|^2 d\Omega \iint_{4\pi} \left| \overrightarrow{E_2}(\theta,\phi) \right|^2 d\Omega}, \quad (1)$$

$$DG = 10\sqrt{1 - (0.99\rho_e)^2}. \quad (2)$$

The calculated ECC and DG results are shown in Figure 16. The ECC during the requiring band is under 0.03 and meets the criterion of 0.5 [33]. The DG is close to its theoretical maximum value of 10 and ensures the outstanding MIMO performance.

Table 1: Structure parameters.

Parameter	Value (mm)
L_1	62.1
L_2	33.6
L_3	23.4
L_4	15.90
L_5	61.1
L_6	28.9
L_7	10.3
L_8	7.4
L_9	41
H_1	1.53
H_2	9.8
W_1	4.8
W_2	45.2
W_3	21.8
W_4	2.30
W_5	1.7
W_6	2.2
W_7	0.5
W_8	0.4
X_1	3.3
X_2	6

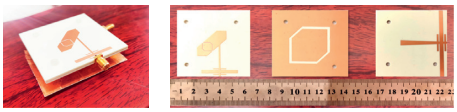

Figure 4: Antenna prototype.

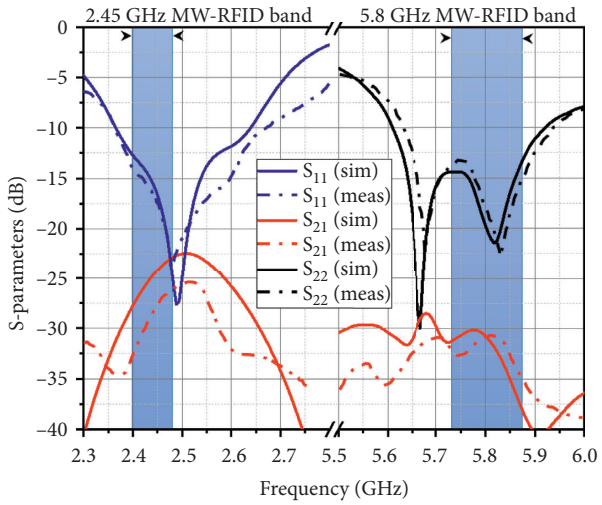

Figure 5: Simulated and measured S-parameters of the antenna.

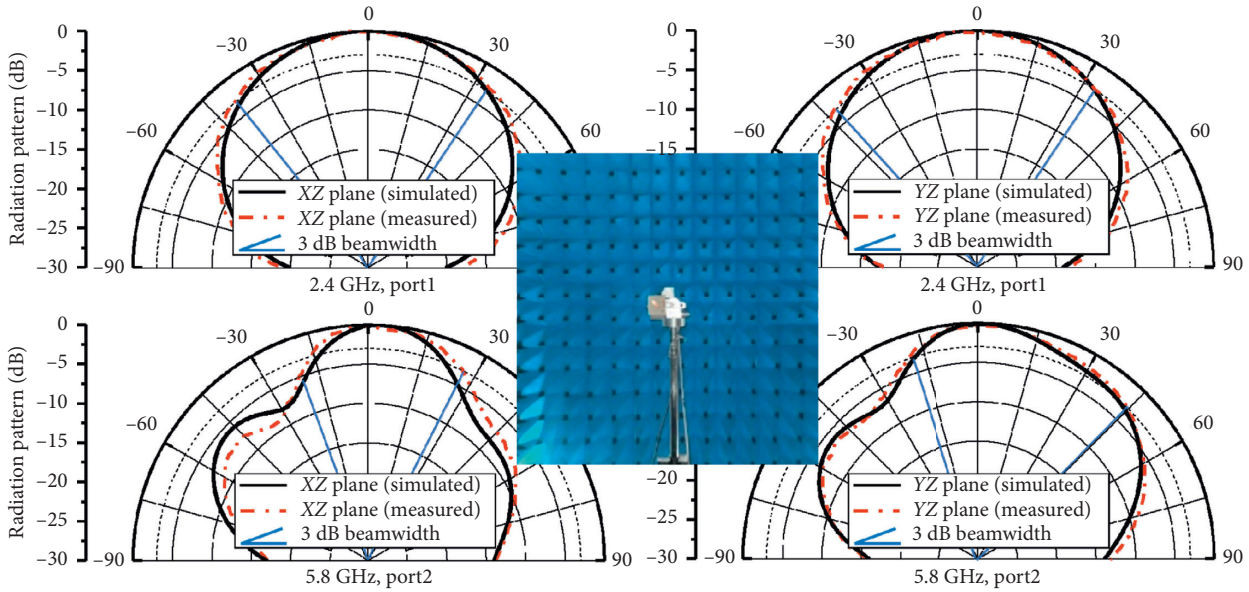

Figure 6: Simulated and measured normalized radiation patterns (RP) at 2.45 GHz and 5.8 GHz in *XZ* and *YZ* planes.

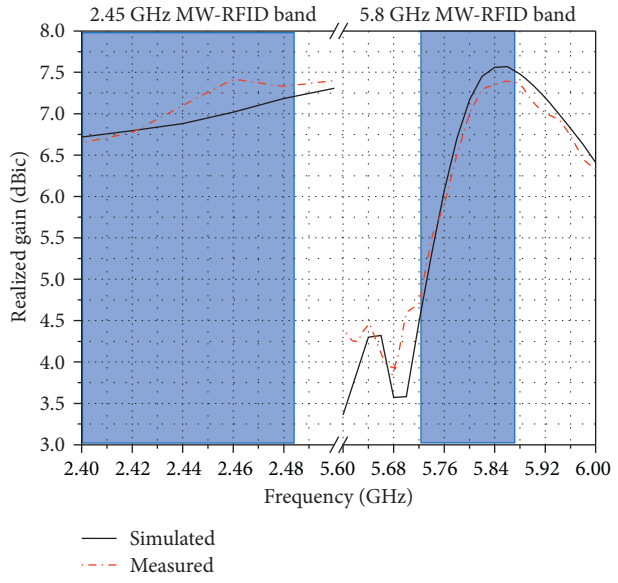

Figure 7: Realized gains in 2.45 GHz and 5.8 GHz MW-RFID band.

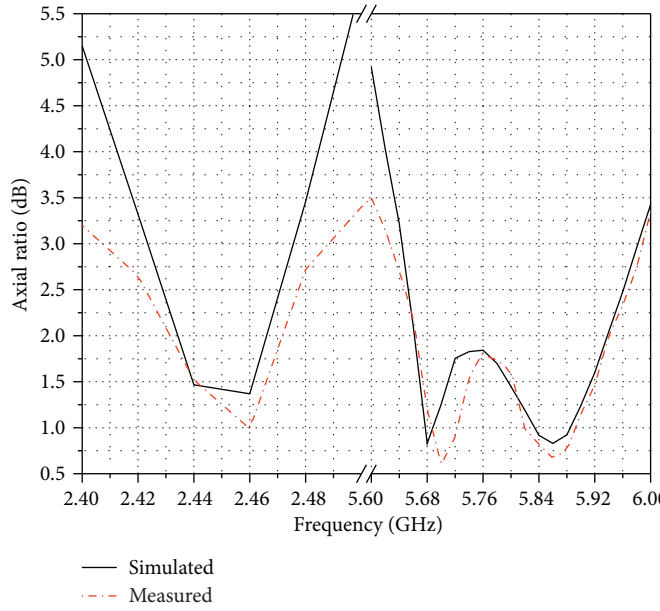

Figure 8: Simulated and measured axial ratio (AR).

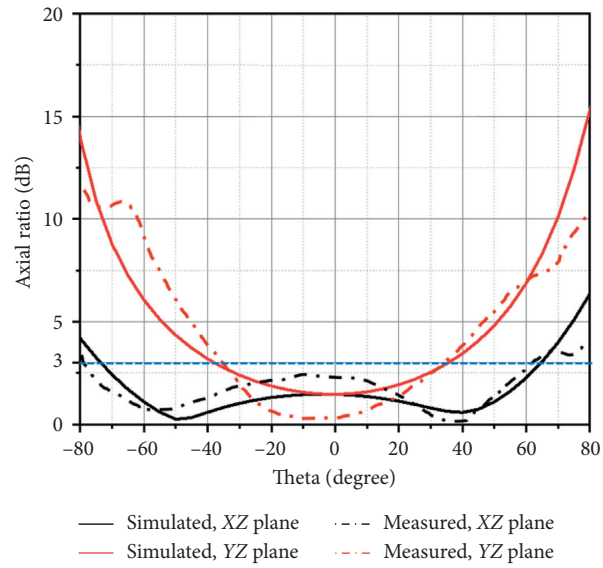

Figure 9: Simulated and measured AR as a function of θ angle from the broadside, in the XZ and YZ planes at 2.45 GHz.

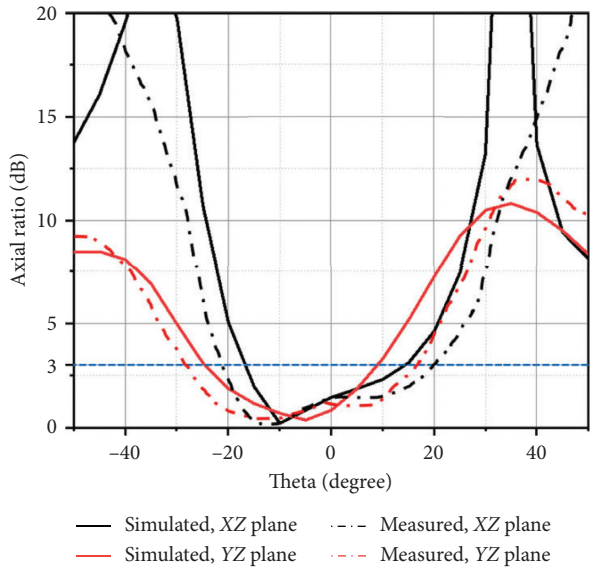

Figure 10: Simulated and measured AR as a function of θ angle from the broadside, in the XZ and YZ planes at 5.8 GHz.

Table 2: Performance comparison with other proposed dual-band dual-port CP antenna systems.

Ref.	Dimensions (λ^3)	Number of radiating elements	Center frequency (GHz)	IMBW (%)	ARBW	Isolation (dB)	Gain (dBic)
[10]	$1.6 \times 1.6 \times 0.5$	8	12 14	16.4 16.7	13.3% 7.4%	20 20	13 13
[11]	$2 \times 2 \times 0.08$	4	5.3 8.2	15.1 9.7	9.4% 6.1%	15 20	13 17
[12]	$1.3 \times 1.3 \times 0.07$	4	7.4 8.1	5 6.2	3.2% 3.7%	25 25	10 10
[13]	$0.9 \times 0.9 \times 0.05$	4	4 5.6	25 15	—	26 26	10 10
[14]	$0.62 \times 0.62 \times 0.1$	2	5.8 7	3.4 3.6	8.6% 1.4%	25 20	5.97 4
[15]	$0.5 \times 0.5 \times 0.05$	5	0.915	2.8	2.8%	25	−0.6
This work	$0.5 \times 0.5 \times 0.11$	1	2.45 5.8	12.7 5.1	3.5% 6.2%	25 30	7.3 7.3

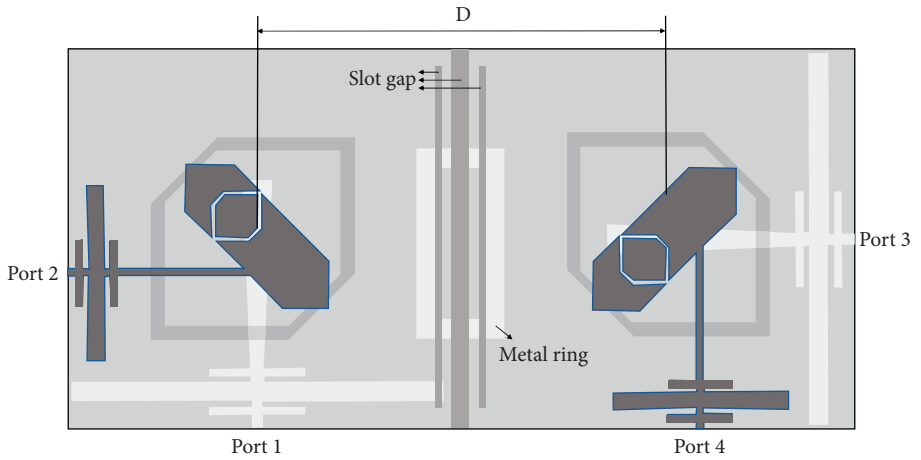

(a)

Figure 11: Continued.

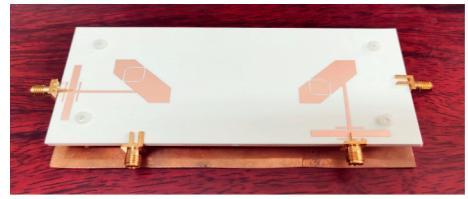

(b)

Figure 11: MIMO antenna layout: (a) top view; (b) fabrication.

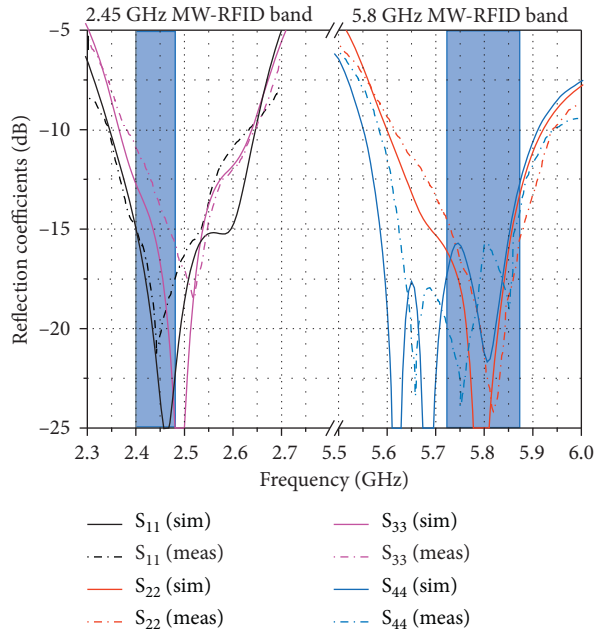

Figure 12: Simulated and measured reflection coefficients.

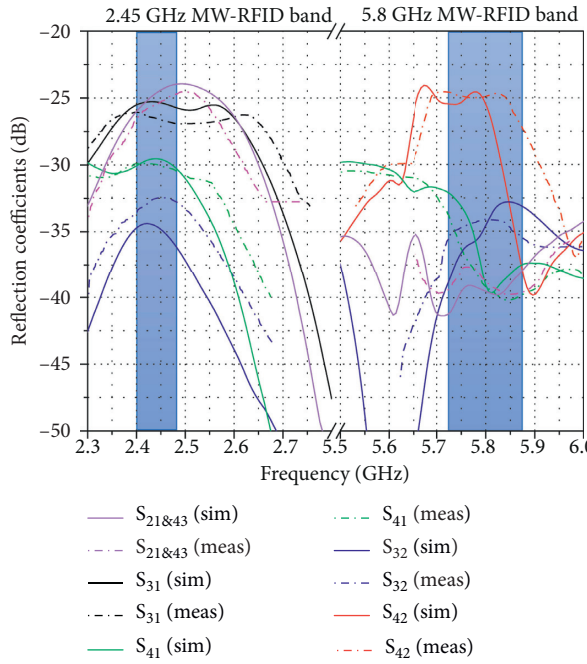

Figure 13: Simulated and measured magnitudes of $S_{21\ \&\ 43}$, S_{31}, S_{41}, S_{32}, and S_{42}.

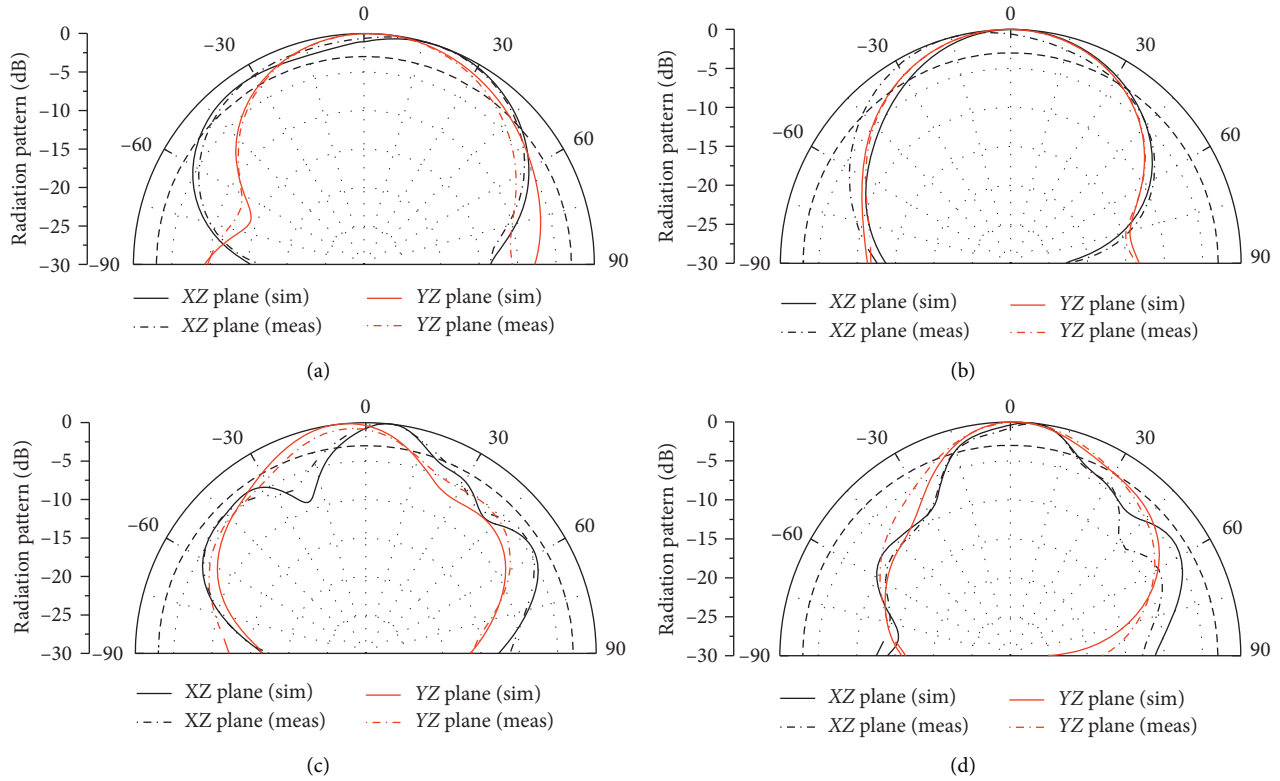

Figure 14: Simulated and measured normalized RP in MIMO configuration. (a) Port 1, 2.45 GHz. (b) Port 3, 2.45 GHz. (c) Port 2, 5.8 GHz. (d) Port 4, 5.8 GHz.

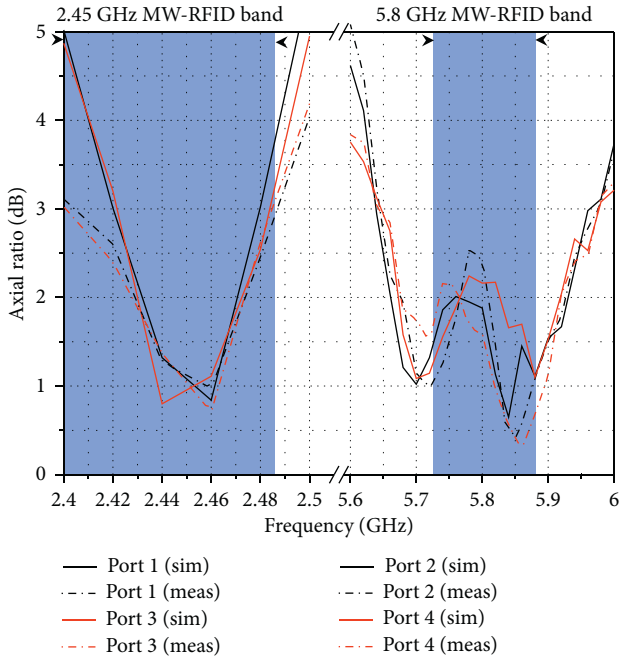

Figure 15: Simulated and measured AR in MIMO configuration.

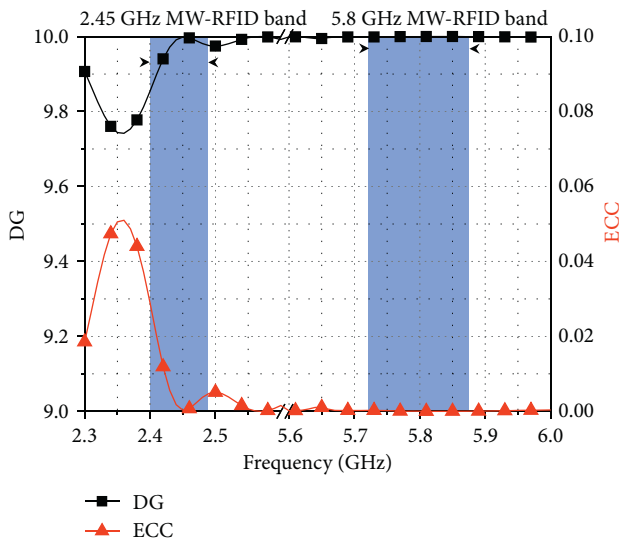

Figure 16: Calculated ECC and DG.

4. Conclusions

A compact, low-profile, dual-port CP antenna for MW-RFID MIMO applications has been designed, prototyped, and characterized. Aperture-shared configuration and DS have been employed to increase the isolation and impedance bandwidth. Moreover, slot gaps and one rectangular metal ring have been adopted to enlarge the ECC. Antenna measurements in terms of S-parameters, AR, RP, realized gain, ECC, and DG agree with numerical results and demonstrate that the proposed prototype is suitable for MW-RFID MIMO application.

Data Availability

The data used to support the findings of this study are available from the corresponding author upon request.

Conflicts of Interest

The authors declare that there are no conflicts of interest regarding the publication of this paper.

Acknowledgments

This work was funded in part by the National Natural Science Foundation of China (Grants nos. 61731007 and U1633202).

References

[1] X. Zhishu and L. Xiuping, "Aperture coupling two-layered dual-band RFID reader antenna design," in *Proceedings of the 2008 International Conference on Microwave and Millimeter Wave Technology*, vol. 3, pp. 1218–1221, Nanjing, China, April 2008.

[2] C. Phongcharoenpanich and R. Suwalak, "Dual-band RFID-reader antenna using annular plate with curved and rectangular slots," in *Proceedings of the 2010 International Conference on Electromagnetics in Advanced Applications*, pp. 633–636, Sydney, Australia, September 2010.

[3] F. Y. Kuo, P. H. Pan, C.-Y. Chiang, H. T. Hsu, and H. T. Chou, "Dual band aperture-coupled patch antenna for RFID mobile terminal applications," in *Proceedings of the 2010 Asia-Pacific Microwave Conference, (APMC)*, pp. 2201–2204, Yokohama, Japan, December 2010.

[4] M. I. Sabran, S. K. A. Rahim, A. Y. A. Rahman, T. A. Rahman, and M. Z. M. Nor Evizal, "A dual-band diamond-shaped antenna for RFID application," *IEEE Antennas and Wireless Propagation Letters*, vol. 10, pp. 979–982, 2011.

[5] B. Huang, Y. Yao, and Z. Feng, "A novel wide beam dual-band dual polarization stacked microstrip dielectric antenna," in *Proceedings of the 2007 International Conference on Microwave and Millimeter Wave Technology*, pp. 1–4, Guilin, China, April 2007.

[6] X. Sun, Z. Zhang, and Z. Feng, "Dual-band circularly polarized stacked annular-ring patch antenna for GPS application," *IEEE Antennas and Wireless Propagation Letters*, vol. 10, pp. 49–52, 2011.

[7] R. K. Vishwakarma, "Design of rectangular stacked microstrip antenna for dual-band," in *Proceedings of the 2009 International Conference on Emerging Trends in Electronic and Photonic Devices & Systems*, Varanasi, India, pp. 22–24, December 2009.

[8] X.-B. Sun, "Circular-slotted microstrip antenna for GPS," *Microwave and Optical Technology Letters*, vol. 52, no. 5, pp. 999-1000, 2010.

[9] H. T. Hsu and T. J. Huang, "Aperture-coupled dual-band circularly polarized antenna for RFID reader applications," in *Proceedings of the 2012 Cross Strait Quad-Regional Radio Science Wireless Technology Conf. (CSQRWC)*, pp. 52–55, New Taipei, Taiwan, July 2012.

[10] S. Ye, J. Geng, X. Liang, Y. Jay Guo, and R. Jin, "A compact dual-band orthogonal circularly polarized antenna array with disparate elements," *IEEE Transactions on Antennas and Propagation*, vol. 63, no. 4, pp. 1359–1364, 2015.

[11] C.-X. Mao, S. Gao, Y. Wang, Q.-X. Chu, and X.-X. Yang, "Dual-band circularly polarized shared-aperture array for C -/X -band satellite communications," *IEEE Transactions on Antennas and Propagation*, vol. 65, no. 10, pp. 5171–5178, 2017.

[12] C.-X. Mao, Z. H. Jiang, D. H. Werner, S. S. Gao, and W. Hong, "Compact self-diplexing dual-band dual-sense circularly polarized array antenna with closely spaced operating frequencies," *IEEE Transactions on Antennas and Propagation*, vol. 67, no. 7, pp. 4617–4625, 2019.

[13] A. B. Smolders, R. M. C. Mestrom, A. C. F. Reniers, and M. Geurts, "A shared aperture dual-frequency circularly polarized microstrip array antenna," *IEEE Antennas and Wireless Propagation Letters*, vol. 12, pp. 120–123, 2013.

[14] L. S. Pereira and M. V. T. Heckler, "Dual-band dual-polarized microstrip antenna for rx/tx terminals for high altitude platforms," in *Proceedings of the 2015 9th European Conference on Antennas and Propagation (EuCAP)*, pp. 1–5, Lisbon, Portugal, April 2015.

[15] R. Caso, A. Michel, M. Rodriguez-Pino, and P. Nepa, "Dual-band UHF-RFID/WLAN circularly polarized antenna for portable RFID readers," *IEEE Transactions on Antennas and Propagation*, vol. 62, no. 5, pp. 2822–2826, 2014.

[16] J. D. Griffin and G. D. Durgin, "Gains for RF tags using multiple antennas," *IEEE Transactions on Antennas and Propagation*, vol. 56, no. 2, pp. 563–570, 2008.

[17] J. D. Griffin and G. D. Durgin, "Multipath fading measurements for multi-antenna backscatter RFID at 5.8 GHz," in *Proceedings of the 2009 IEEE International Conference on RFID*, pp. 322–329, Orlando, FL, USA, April 2009.

[18] S. Sabesan, M. Crisp, R. V. Penty, and I. H. White, "An error free passive UHF RFID system using a new form of wireless signal distribution," in *Proceedings of the 2012 IEEE International Conference on RFID (RFID)*, pp. 58–65, Orlando, FL, USA, April 2012.

[19] R. Langwieser, C. Angerer, and A. L. Scholtz, "A UHF frontend for MIMO applications in RFID," in *Proceedings of the 2010 IEEE Radio and Wireless Symposium (RWS)*, pp. 124–127, New Orleans, LA, USA, January 2010.

[20] D. Ma and W. X. Zhang, "Broadband CPW-Fed RFID antenna at 2.45/5.80 GHz," in *Proceedings of the 2007 International Workshop on Anti-counterfeiting, Security and Identification (ASID)*, pp. 84–87, Xizmen, China, April 2007.

[21] A. T. Mobashsher, M. T. Islam, and N. Misran, "A novel high-gain dual-band Antenna for RFID reader applications," *IEEE Antennas and Wireless Propagation Letters*, vol. 9, pp. 653–656, 2010.

[22] A. Sharma, I. J. G. Zuazola, and A. Perallos, "Multipurpose near- and far-field switched multiband coil antenna for 915-MHz/2.45/5.8-GHz RFIDs," *IEEE Antennas and Wireless Propagation Letters*, vol. 16, pp. 2562–2565, 2017.

[23] A. T. Mobashsher and R. W. Aldhaheri, "An improved uniplanar front-directional antenna for dual-band RFID readers," *IEEE Antennas and Wireless Propagation Letters*, vol. 11, pp. 1438–1441, 2012.

[24] D. M. Pozar, "Microstrip antenna aperture-coupled to a microstrip-line," *Electronics Letters*, vol. 21, no. 4, pp. 49-50, 1985.

[25] R. Garg, P. Bhartia, I. J. Bahl, and A. Ittipiboon, *Microstrip Antenna Design Handbook*, Artech House, Boston, MA, USA, 2001.

[26] R. Caso, A. A. Serra, M. Pino, P. Nepa, and G. Manara, "A wideband slot-coupled stacked-patch array for wireless communications," *IEEE Antennas and Wireless Propagation Letters*, vol. 9, pp. 986–989, 2010.

[27] R. Caso, A. Serra, A. Buffi, M. Rodriguez-Pino, P. Nepa, and G. Manara, "Dual-polarised slot-coupled patch antenna excited by a square ring slot," *IET Microwaves, Antennas & Propagation*, vol. 5, no. 5, pp. 605–610, 2011.

[28] R. Caso, A. Buffi, M. Rodriguez Pino, P. Nepa, and G. Manara, "A novel dual-feed slot-coupling feeding technique for circularly polarized patch arrays," *IEEE Antennas and Wireless Propagation Letters*, vol. 9, pp. 183–186, 2010.

[29] A. Buffi, R. Caso, M. R. Pino, P. Nepa, and G. Manara, "Single-feed circularly polarised aperture-coupled square ring slot microstrip antenna," *Electronics Letters*, vol. 46, no. 4, pp. 268-269, 2010.

[30] E. Zhang, A. Michel, M. R. Pino, P. Nepa, and J. Qiu, "A dual circularly polarized patch antenna with high isolation for MIMO WLAN applications," *IEEE Access*, vol. 8, pp. 117833–117840, 2020.

[31] N. Llombart, A. Neto, G. Gerini, and P. de Maagt, "Planar circularly symmetric EBG structures for reducing surface waves in printed antennas," *IEEE Transactions on Antennas and Propagation*, vol. 53, no. 10, pp. 3210–3218, 2005.

[32] M. Y. Jamal, M. Li, and K. L. Yeung, "Isolation enhancement of closely packed dual circularly polarized MIMO antenna using hybrid technique," *IEEE Access*, vol. 8, pp. 11241–11247, 2020.

[33] U. Ullah, I. B. Mabrouk, S. Koziel, and M. Al-Hasan, "Implementation of spatial/polarization diversity for improved-performance circularly polarized multiple-input-multiple-output ultra-wideband antenna," *IEEE Access*, vol. 8, pp. 64112–64119, 2020.